2013-06-12

Hall-Effect in an eight-shaped conductor

Cedric Ranjit Singh SODHI

Filed as B.Sc. thesis at the *IQI* of the *RWTH Aachen University*, mentored by *Prof. David DiVincenzo*

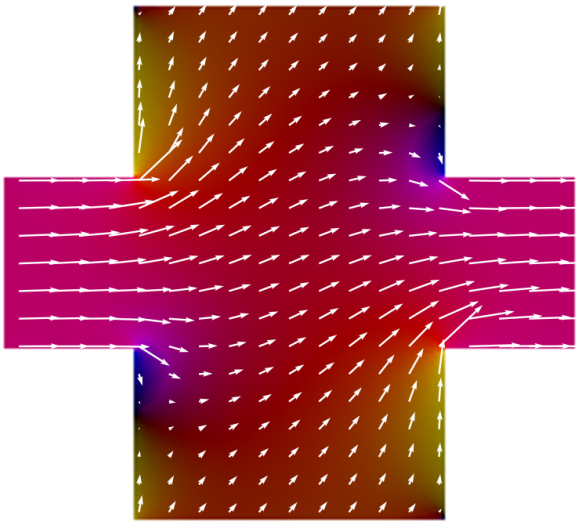

Table of contents

1. Introduction

A *Gyrator*, as originally defined by B. D. H. Tellegen in his 1948 paper *THE GYRATOR, A NEW ELETRIC NETWORK ELEMENT* is a theoretic, **two port** electric network element, characterized by its **resistance matrix**

$$Z = \begin{bmatrix} 0 & R \\ -R & 0 \end{bmatrix}$$

which implies that the Gyrator is an ideal, lossless, **non-reciprocal** element. *Two port elements* are a subset of network elements with four connecting terminals, which are grouped in pairs, each of which satisfies a condition, that the net current into the two associated terminals sums to zero. Therefore, the overall charge in the element is conserved. The gyrator is a special element among those, in that it is non-reciprocal, which may come about due to a variety of conditions which prevent application of **reciprocity theorems**, known as *Lorentz reciprocity* in the time-harmonic case (e.g. for transformers), *Green's reciprocity* in electrostatic problems or more specific versions for particular scenarios.

Reciprocity theorems state, coarsely, that, under certain prerequesites, cause and effect in electromagnetics are dual to eachother in that they may be interchanged. Tellegen, in his paper, illustrates *Green's reciprocit* for an energy-conserving electrostatic two-port element consisting of two lossless insulated conductors. Obviously, a very simple example. Pathologic to the point where it is useless. Similarly, the more general reciprocity theorems for *Lorentz-* and *Green's reciprocity* make much stronger assumptions and are rarely applicable to real electronics.

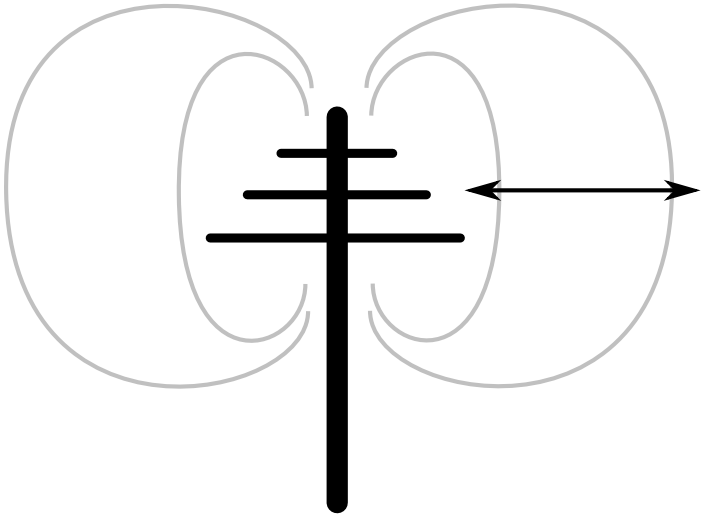

<1>: An antenna is a prototypical example for a *Lorenz-reciprocal* system. An specific antenna receives a kind of signal as well as it sends it.

It is therefore little surprising that it turns out to be possible to conceive *two port*, or more generally *four terminal* elements which violate reciprocity (are *antireciprocal*) or are even completely *nonreciprocal*, such as the Gyrator, as it was proposed by Tellegen.

Perhaps the most famous of such elements is the *Hall effect gyrator* which, despite its name, is “only” antireciprocal rather than nonreciprocal. As the name suggests, the *Hall-Effect gyrator* makes use of the electrostatic Hall effect and more particularly of the peculiar antisymmetry of the cross-product governing the dynamics of charges in a magnetic field. Charges moving in a constant magnetic field fail to satisfy the requirements for *Lorentz reciprocity* and are not applicable to *Green's reciprocity* at all, to name the two major reciprocity relations.

From the behaviour of the Hall-Effect, it is clear that applying a current-inducing voltage U_A across a Hall bar, port *A*, one obtains a voltage U_B and thus possibly a current I_B perpendicular to the magnetic field $B \in \mathbb{R}^3$ and the current, over the other port *B*. This is the effect which is used by *Hall sensors*. The sign of the resulting voltage depends, apart from an arbitrary choice of polarity, on the **right-hand rule**, i.e. the properties of the cross product. This is because the magnetic force $F \in \mathbb{R}^3$ on the charge-carriers with charge $q \in \mathbb{R}$ and speed $v \in \mathbb{R}^3$ behaves like

$$F = qv \times B$$

or, in the continuum mechanical case, which we consider here

$$\mathfrak{F} = \rho\,(E + v \times B)$$

where $\rho \in \mathbb{R}$ is the charge density and $\mathfrak{F} \in \mathbb{R}^3$ the according force density. If polarities are chosen such that a positive current across port *A* results in a positive potential across port *B*, then, reversing the situation, a positive current across port *B* will cause a **negative** potential across *A*, antireciprocity is achieved.

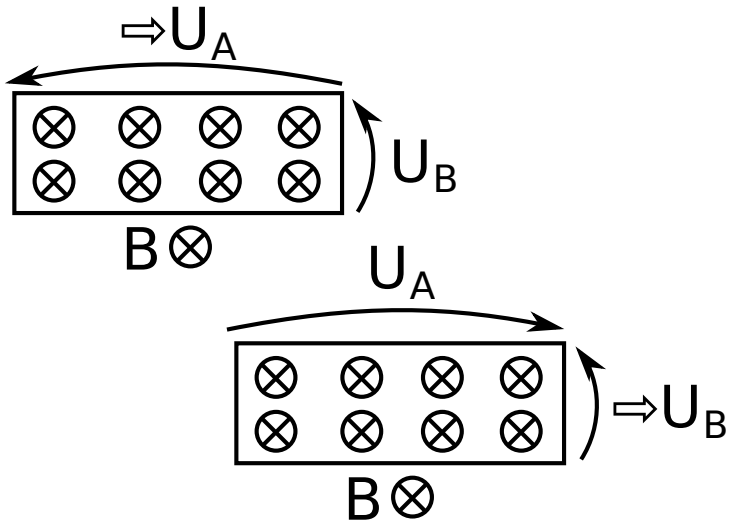

<*2*>: In the Hall bar, exchanging driving voltage and resulting voltage has a similar effect like reversing the magnetic field. The relative sign between the two changes.

1.1. On notation

The syntax in this report follows **functional notation** (as opposed to the notoriously ambiguous *systematic* notation commonly found in physics) where any symbol which may take arguments like a function **is** a function in these arguments. **Example:** $E(x,y,z)$ and $E(\xi,\eta,\zeta)$ refer to the same function, i.e. they return the same value for the same arguments. Also, $\partial E / \partial x$ is ill-defined, so is $\partial E(\xi,\eta,\zeta) / \partial x$.

For the sake of orientation, the report attempts to name placeholders according to what "*plane*" they "live" in – for example $u \in \mathbb{D}$ – but the reader should not rely on this and be prepared for exceptions, for instance when names would collide.

If a function is to be derived with respect to an argument which, after differentiation, is set to a specific value – something commonly denoted by "vertical bar notation" – it will be noted as

$$\frac{\mathrm{d}f}{\mathrm{d}x}(x=g(y)) \equiv \frac{\mathrm{d}f}{\mathrm{d}[g(y)]}(g(y))$$

Arguments to symbols may be surpressed in relational statements. That implies that all non-constant symbols match their arguments in order.

Example: Given a proper definition of the respective symbols, where each takes four distinct parameters

$$B_i \equiv \nabla \times A$$

equates to

$$B_i(t,x,y,z) \equiv \nabla \times A(t,x,y,z)$$

Similarly, surpressing arguments for functional symbols which take a different number or order of arguments is ill-defined and wrong, respectively.

Further, we shall use the symbol $\doteq$ for substitutions (similar to *systematic* notation), where a symbol is to be understood as bound to an alias for other symbol(s) without noting dependence on the latter explicitly. **Example:** $k \doteq k(\rho(x,y,z))$ will shorten equations in that we can write something like

$$\nabla \cdot j = kR \nabla \cdot E$$

instead of

$$\nabla \cdot j(x,y,z) = k(\rho(x,y,z))R \nabla \cdot E(x,y,z)$$

This is an example for substitution and “subsequently” surpressed arguments to all involved functions.

2. Statement of the problem

The goal of this thesis is to find a numerical solution to the Hall-effect in an eight-shaped conductor. The driving potential for the current in one of the loops arises from a **constantly changing magnetic field** through that loop. A couple of reasonable simplifications on the shape of the conductor and the acting magnetic field are assumed, in order to reduce the problem to its interesting characteristics, namely those of the eight's intersection and the amount of non-reciprocity obtained. These simplifications are

- The eight is formed from two infinitely thin conductors which intersect at $90°$, much like two strips of paper, which are formed to rings and glued together in a $90°$ with respect to eachother. This permits treatment on a two-dimensional domain, specifically on $\mathbb{C}$.
- The static magnetic field is assumed to penetrate the surface of the structure with a fixed strenghth perpendicularly and in a single orientation. This suggests that self-inductivity of the conductor is neglected and that the conductor can be sufficiently shielded from

inhomogenities. Whereas it can be argued that the effect of the magnetic field induced by other parts of the condutor on itsself vanishes in the limit of large radii, it is not immediately apparent why self inducitivity over the breadth of a piece of the conductor could be ignored. In fact, the resulting "*self*" *Hall effect* in a piece of the strip due to the magnetic field induced by an adjacent current density is proportional to the current in the strip. However, if we choose the static field to be sufficiently large, the current can be choosen accordingly small (because the Hall-Effect is proprotional to the product of current and magnetic field). Hence, the effect of self-induction can be made negligibly small in comparison to the Hall-Effect due to the static field.

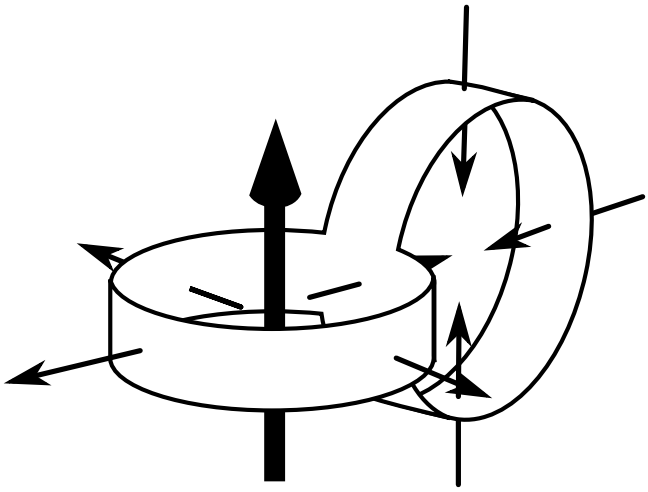

<*3*>: The conductor consists of two very thin strips which are formed into loops and glued onto eachother. Both loops are homogenously embedded in a static magnetic field (thin arrows) and one of the loops is pierced by a changing magnetic field (thick arrow).

- The changing magnetic field is modelled by its effect on the electric field in the conductor.
- The conductor is Ohmic and anisotropic, i.e. current and Lorentz force are related by a fixed scalar, the resistivity $R \in \mathbb{R}$.

2.1. Simplifying assumptions for the field equations

The assumption that the conductor behaves Ohmic bears subtle, yet strong implications beyond just the obvious. A first step towards that conclusion is to realize that it is not immediately clear what the symbols in

Ohm's law refer to.

In the purely electric case, where it states $E = Rj$, it gives a **macroscopic phenomenological** description of the relation between the electric field and the current j and thus predicts how much electric charge moves per volume and time.

The way Ohm's law is phrased, it **postulates** an **instantaneous relation** between the Lorentz force and the current. Mathematically, the Newtonian differential equations of motion, which somehow relate the substantial time derivative (also known as *convective derivative* in fluid mechanics) of j

$$\frac{\mathrm{D}j}{\mathrm{D}t} = \left(\frac{j}{\rho} \cdot \nabla\right) j$$

to the acting forces is collapsed at zero mass and the freedom inherent to the solution of a differential equation disappears, as does the notion of any fields which constitute j.

Now consider the Ohmic equation extended by the term for the magnetic force

$$Rj = E + v \times B \tag{1}$$

which holds in equilibrium when the forces which cancel out the Lorentz force are collected in a "*drag*"-like term $R\rho j$ like

$$\underbrace{\rho R j}_{\text{drag force}} = \rho\,(E + v \times B)$$

and by assuming it holds **everywhere**, we consequently assume that equilibrium is reached everywhere and thus instantly along the flow lines of j.

Whereas the original law without a magnetic field made an empiric statement regarding macroscopic observables **without** notion of any mechanism of flowing charges, the "extended" version introduces v, a new, third quantity which somehow refers to the underlying mechanism of **moving** charges. However, it does not tell us how exactly v is related to j. It is up to us to model a relation between v and j which is consistent with physical reality. The obvious question to ask here is what exactly v is defined to be.

The naive answer $j = \rho v$ gives no insights, it just shifts the question from "*What is v?*" to "*What is ρ?*". Identifying ρ with that in Maxwell's first equation, commonly denoted as $\nabla E = \rho / \varepsilon_0$ leads to a physical

contradictions such as predicting the current is zero if there is no net charge. We now introduce the following set of assumptions to reconcile the notion of ρ and j with our expectations:

- Ohm's extended law describes a current j which is constituted by a charge field ρ. The physical charge field is a superposition of a constant charge ρ_0 and ρ.

In that sense, ρ represents **mobile** charges, which abide to Ohm's law, on top of a **stationary background** ρ_0 which Ohm's law has no notion of.

The direct dependence of j on E and B also rules out the effect of other interacting forces and, most important, any **depletion of charges**. The mechanism by which charges are disabled from crossing the boundary of the conductor must thus be included in a suitable E. This is reflected by the boundary condition for E in the mathematical description of the problem, which is given later.

3. Outline of the solution

The respective loops of the eight are cut opened and layed out flat as a simply connected domain onto the complex plane. The problem is then restated in terms of a scalar potential for the electric field E on $\mathbb{C}$. Following the ideas of R. F. Wick in the 1953 report *Solution of the Field Problem of the Germanium Gyrator*, a solution for an electric scalar potential $\phi(x, y)$ in the conductor is obtained which satisfies the boundary constraints of the problem on $\mathbb{C}$. The solution is finally transformed back onto the triply-connected submanifold in the original problem domain $\mathbb{R}^3$.

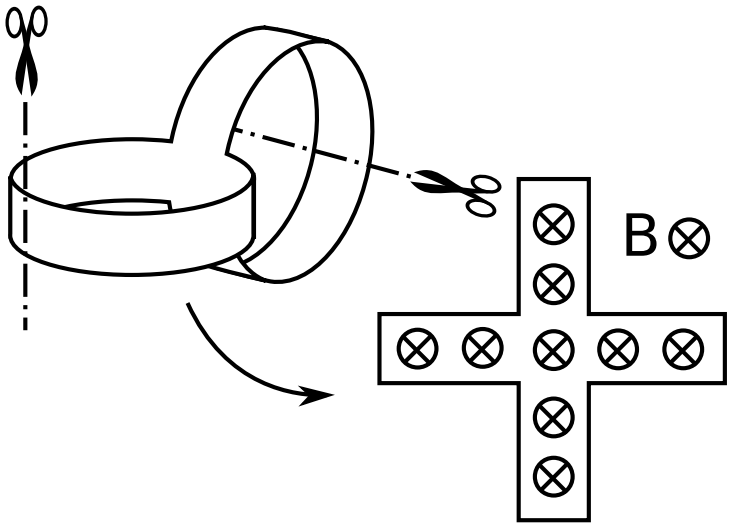

<4>: Outline of the solution: Consider the problem in the submanifold which describes the conductor and solve it in the according two-dimensional space.

4. Situation of the conductor in fields and potentials

We shall call the loop into which the power is injected by means of Faraday's law the *primary loop* and the other the *secondary loop*, respectively. The *intersection* shall be called exactly that. The origin of the three-dimensional coordinate-system used shall be placed in the center of the primary loop. The x-axis (coordinate x) shall be orthogonal to the intersection's surface pointing away from the intersection, the z-axis (coordinate z) parallel to the surface of the primary loop. The y-axis (coordinate y) is oriented so to obtain a right-handed coordinate-system.

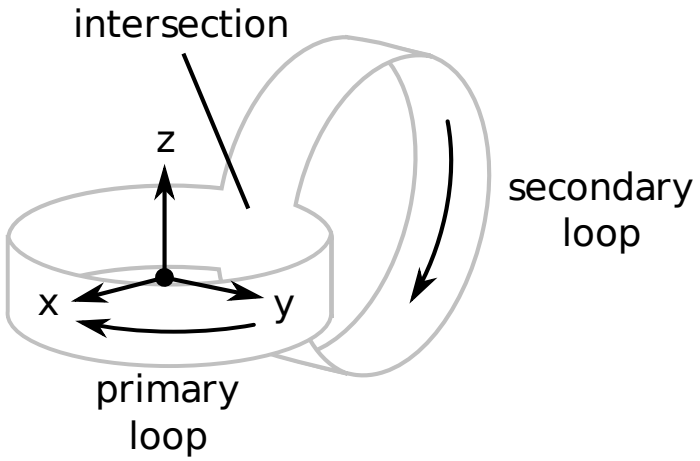

<5>: The center of the three dimensional coordinate system – which is only relevant for describing the problem – is placed in the center of the primary loop.

4.1. Injection of power by induction

Instead of applying a driving potential across two distinct terminals in one of the loops, **induction** is used to supply the system with power. More specifically, we assume that the hole formed by the primary loop is pierced by a magnetic field $B_i \in \mathbb{R}^3$ which constantly changes by $b \in \mathbb{R}^3$ with time t

$$B_i(t,x,y,z) \equiv tb(x,y) \tag{2}$$

and is taken to be independent of z. By *Stokes*' *theorem* this relates to the voltage over the curve integral through the primary loop ∂L_1 by

$$\oint_{\partial L_1} d\gamma(x,y,z) \cdot E(x,y) = \int_{L_1} d\sigma(x,y,z) \cdot b(x,y)$$

Because of the independence of z, the electric field resulting from B_i is the same for all z. We now want to construct B_i so that it does **not** induce a

voltage across the secondary loop, creates a **constant** electric field in the primary loop and does **not** effect a magnetic force on charges in the conductor, i.e. doesn't interfere with the static magnetic field. The electric field resulting from the magnetic field is encoded in the associated vector potential $A \in \mathbb{R}^3$

$$B_i \equiv \nabla \times A$$

by

$$E = \nabla \cdot \phi + \dot{A} \tag{3}$$

We thus want the projection of $\dot{A}$ onto the surface of the primary loop to be constant along that surface. In order to satisfy the second and third requirement, $\dot{A}$ needs to be a fixed value for all points on the secondary loop and consequently take the value of intersection, which is part of it.

This implies that the effect of B_i can not be isolated to the primary loop and can be illustrated as follows: If $\dot{A}$ or its projection is constant on the primary loop, that will include the intersection, which, for simplicity, we consider flat for the moment. If $\dot{A}$ was to vanish in the secondary loop, this would imply $\nabla \times \dot{A} \neq 0$ as we move from the intersection outwards into the region of the secondary loop. Since $\nabla \times \dot{A} \neq 0$ implies $\dot{B} \neq 0$, this would result in a magnetic field component perpendicular to the conductor and thus interfere with the static magnetic field.

However, the necessary electric field in the secondary loop lies in the surface and is perpendicular to the border. It does therefore not constitute a driving voltage, and does not affects the solution to the problem.

This, and the condition that B shall not effect a magnetic force motivates the exact form of

$$A_1(t, x, y, z) \equiv \frac{1}{2} b_0 t \begin{bmatrix} y \\ -x \\ 0 \end{bmatrix}$$

$$A_2(t, y, y, z) \equiv \frac{1}{2} b_0 t \begin{bmatrix} 0 \\ R_1 \\ 0 \end{bmatrix}$$

where R_1 denotes the distance of the intersection from the origin, i.e. the radius of the primary loop, in

$$A(t, x, y, z) \equiv \begin{cases} A_1(t, x, y, z) & x \geq -R_1 \\ A_2(t, x, y, z) & \text{else} \end{cases}$$

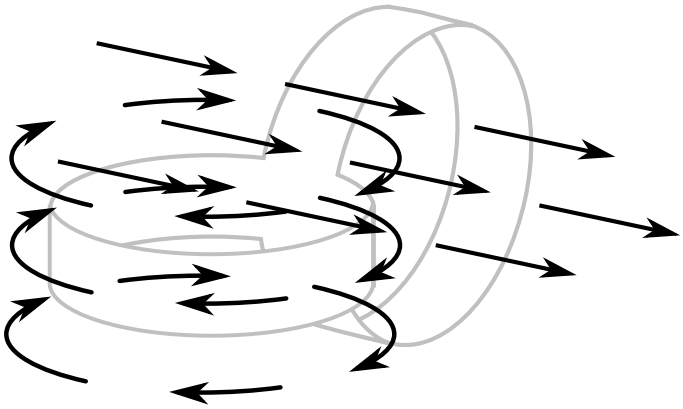

<6>: The vector potential A is circulating along the primary loop and is constant and parallel to the surface everywhere on the secondary loop.

This will guarantee $B_i = \nabla \times A = 0$ for every point on the secondary loop. Although we do not need to make any statement about the exact form of A on the interior of the loop's respective holes, this definition proves that an A can be chosen which corresponds to the assumed form *(2)* of the driving magnetic field with, in this case

$$b(x,y) = \begin{bmatrix} 0 \\ 0 \\ 1 \end{bmatrix} \begin{cases} b_0 & x \geq -R_1 \\ 0 & \text{else} \end{cases}$$

Note that B_i does not actually vanish on the primary loop but lies parallel to the surface and thus exerts no magnetic force on the strip, which we take to be a two-dimensional submanifold.

5. Governing differential equations

The proposed setup of static magnetic field B, the driving field B_i, the assumption of Ohm's law *(1)*, and the geometry of the conductor can be combined into a single **Laplacian differential equation** with boundary conditions for a potential of the electric field E on $\mathbb{R}^3$ and from there onto the complex plane.

In order to find the consequence of Ohm's law in terms of the desired problem domain $\mathbb{C}$, we examine its consequence in Euclidean $\mathbb{R}^3$, where it is formulated and transform that result into the submanifold. The advantage of this approach over the vague argument that the conductor was sufficiently flat locally is that the necessary approximations become explicit.

We take the magnetic force due to B_i *a priori* compensated for by a force which might be noted $E_\perp \in \mathbb{R}^3$. This force is considered electric, although its origin – electric or not – may remain unaccounted for. Equation *(1)* on the conductor does then not include B_i, can be solved for j and rewritten to:

$$j = k\left(RE - \frac{1}{\rho} B \times E\right) \tag{4}$$

where

$$k \doteq k(\rho) \equiv \frac{1}{R^2 + \left(\frac{B}{\rho}\right)^2}$$

We know $\nabla \cdot j = 0$ in the sought stationary case. Applying the divergence yields

$$\begin{aligned} \nabla \cdot j &= k \nabla \cdot \left[RE - \frac{1}{\rho} B \times E\right] + (RE - \frac{1}{\rho} B \times E) \cdot \nabla k \\ &= k\left(R \nabla \cdot E - \frac{1}{\rho}(E \cdot (\nabla \times B) - B \cdot (\nabla \times E)) - (B \times E) \nabla \frac{1}{\rho}\right) + \\ &\quad \left(RE - \frac{1}{\rho} B \times E\right) \nabla \cdot k \end{aligned}$$

B changes only as slowly as to follow the conductor perpendicularly and is thus approximately constant, $\nabla \times E = 0$ in the time stationary case, so both terms vanish.

$$\nabla \cdot j = kR \nabla \cdot E - (B \times E) \cdot \nabla \frac{k}{\rho} + RE \nabla k$$

With

$$\nabla \frac{k}{\rho} = \left(k + 2\left(\frac{Bk}{\rho}\right)^2\right) \nabla \frac{1}{\rho}$$

it follows, that

$$\frac{1}{k} \nabla \cdot j = R \nabla E - \left(2RB^2 \frac{k}{\rho^3} \nabla \rho + \left(\frac{1}{\rho^2} + 2B^2 \frac{k}{\rho^5}\right) B \times \nabla \rho\right) \cdot E \tag{5}$$

Replacing ρ with the assumption that

$$\nabla \cdot E = \frac{\rho + \rho_0}{\varepsilon_0}$$

in Maxwell's first equation and requiring that $\nabla \cdot j = 0$ leads to a differential equation for E, the **governing differential equation**. This is a partial differential equation of 2nd order to the 6th power of the involved

derivatives on a triply connected domain.

5.1. Boundary conditions, existence and uniqueness of the solution

The problem on the conductor's domain in $\mathbb{R}^3$ is constrained by the following conditions, which we infer from physical necessity:

1. The conductor be overall neutral. That is, the integral of $\nabla \cdot E$ over its domain is zero.

2. The current j at the border be parallel to that border.

3. ρ is strictly of one sign. By the first constaint, that implies it has the opposite sign of ρ_0. This is then an appropriate model for a single species of charge carriers.

4. The voltage along the primary loop agrees with the externally induced voltage.

5. The voltage along the secondary loop vanishes, because by construction, the flux through that loop is time-constant.

Given the nature of the differential equation we're not able to readily make statements about the existence or uniqueness of a solution in advance. It is not clear whether the model permits a solution which satisfies said constraints. It should also be noted that it is not necessarily safe to assume that, even if Ohm's law permits a solution, the approxiations we have made are still consistent, too. Similarly, the uniqueness of a solution, if it exists, for the imposed boundary conditions is not proven, either.

Existence of a solution, however, be made plausible analytically, by noting that $\rho = -\rho_0$ satisfies both, constraint 1 and 3. Under this assumption, equation *(5)* reduces to

$$\nabla \cdot E = 0 \tag{6}$$

6. Remapping from R^3 to R^2

The two loops are cut open at the respective points opposite to the intersection and the resulting, simply connected submanifold together with the associated projection of the fields $\dot{A}$ and E **isometrically** mapped by the according cross-like domain $K \subset \mathbb{R}^2$.

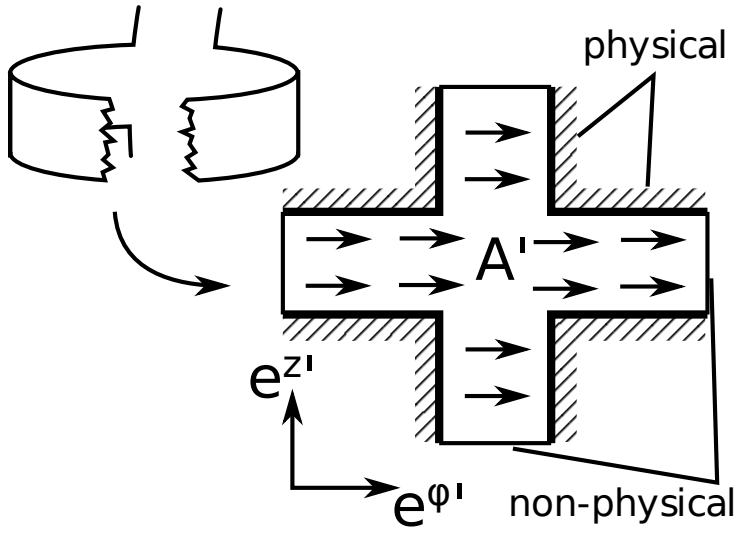

<7>: When the conductor is cut open and layed out flat on the table and the projection of A is considered, it will be a constant everywhere.

The boundaries of this domain which correspond to the **physical** boundaries of the conductor are henceforth referred to as *physical edges*, whereas those arising from the two respective **cuts** are called the *non-physical edges*.

The offset in the plane is to be specified later, when the mapping in the complex plane is considered. For now, the orientation is chosen such that **at the intersection** the horizontal axis $e^{\phi\prime} \in \mathbb{R}^2$ goes along the primary loop and the virtual axis **into** the plane $e^r \in \mathbb{R}^3$ goes outwards along the radius of the primary loop. The vertical axis of the chart $e^{z\prime} \in \mathbb{R}^2$ consequently follows the secondary loop.

As the naming suggests, this choice partially corresponds to the normalized, natural local coordinates of an appropriately aligned cylindrical coordinate system along the primary loop. We denote the transformation into the corresponding local coordinates by the tensor e^{μ}_{ν}, the projected electric field by E'^{μ} and the renormalized coordinate vector by

$$c(\varphi, z, r) \equiv R \begin{bmatrix} r\cos\frac{\varphi}{R} \\ r\sin\frac{\varphi}{R} \\ \frac{z}{R} \end{bmatrix}$$

which yields e^r, e^{ϕ}, and e^z and guarantees orthonormality $e^{\mu}_{\rho} e^{\rho}_{\nu} = \delta^{\mu}_{\nu}$ in the submanifold. The divergence of E' (with respect to the chart's coordinates) is then

$$\begin{aligned}\partial_\mu E'^\mu &= E'^\nu \partial_\mu e_\nu^\mu + e_\nu^\mu \partial_\mu E'^\nu \\ &= E'^\nu \partial_\mu e_\nu^\mu + e_\nu^\mu (\partial_\rho E^\nu)(\partial_\mu c^\rho) \\ &= E'^\nu \partial_\mu e_\nu^\mu + e_\nu^\mu (\partial_\rho E^\nu) e_\mu^\rho \\ &= E'^\nu \partial_\mu e_\nu^\mu + \delta_\nu^\rho (\partial_\rho E^\nu)\end{aligned}$$

where the last two lines follow by isometry and orthonormality, respectively. From the geometry of the submanifold, i.e. $c(\varphi, z, r)$ it follows that

$$\partial_r e_\nu^r(\varphi, z, r) = \partial_z e_\nu^z(\varphi, z, r) = 0$$

and

$$\partial_\varphi e^\varphi(\varphi, z, R) = -\frac{1}{R}\begin{bmatrix} \cos\frac{\varphi}{R} \\ \sin\frac{\varphi}{R} \\ 0 \end{bmatrix}$$

which vanishes for sufficiently large R. That means, if the primary loop is sufficiently flat, the divergence in local coordinates is equal to the divergence in eucledian $\mathbb{R}^3$ and further, if the derivative of E along e^r is small, it is equal to the two-dimensional divergence in the chart. The same derivation can be analogously applied to the **secondary loop**, so that it holds for the conductor as a whole. Therefore, it follows from *(6)* that

$$\nabla \cdot E' = 0$$

on $\mathbb{R}^2$.

By a reasoning similar to *(7)* it can be shown that if there exists a $\phi : \mathbb{R}^3 \to \mathbb{R}$ so that

$$E = \nabla\phi + \dot{A}$$

in eucledian space, there always exists a $\phi' : \mathbb{R}^2 \to \mathbb{R}$ so that

$$E' = \nabla\phi' + \dot{A}'$$

where A' is the projected A:

$$\begin{aligned}E'^\mu = e_\nu^\mu E^\nu &= e_\nu^\mu \partial^\nu \phi + e_\nu^\mu \dot{A}^\nu \\ &= (\partial_\nu c^\mu)(\partial^\nu \phi) + \dot{A}'^\mu \\ &= \partial^\mu \phi' + \dot{A}'^\mu\end{aligned}$$

of which we only consider two components in the tangent space. Given the

nature of $\dot{A}'$ which, by construction is constant everywhere on the chart

$$\dot{A}' = \frac{1}{2} R b_0$$

and can therefore be expressed as the gradient of a scalar field $\alpha' \in \mathbb{R}$, E' can in turn be expressed as the gradient of a potential $\psi' \in \mathbb{R}$

$$E' = \nabla (\phi' + \alpha') \equiv \nabla \psi' \qquad (8)$$

implying $\nabla \times E' = 0$, and is subject to the following boundary conditions:

1. The current resulting from the field at the boundary which is mapped to the **physical** boundary of the conductor ought to be parallel to the boundary. By virtue of equation *(4)* and the assumption that ρ is constant, E and j enclose a constant angle at every point. The condition is therefore satisfied if E' makes an equivalent angle of

   $$\gamma \equiv arctan\left(-\frac{\rho_0 R}{|B|} \right) \pm \frac{\pi}{2}$$

   the s.c. *Hall angle* with the boundary

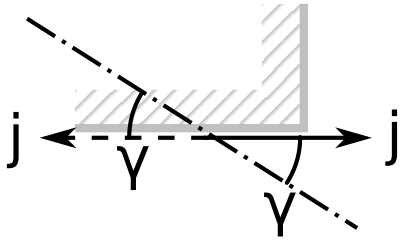

   <8>: The s.c. *Hall angle* is the angle which is enclosed between the direction of the electric field and the current. Because the current can not pass over the boundary of the conductor and because the Hall angle is constant, the electric field at the boundary has to point in either of two possible directions.

2. The field transit smoothly across the non-physical edges of the cross, at which we mean to “glue” the loops back together, that is

   $$E'(s) = E'(f)$$

where s and f denote two corresponding points on the two respective non-physical edges of each loop.

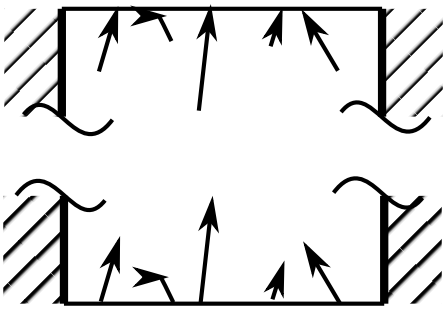

<*9*>: In three dimensions we have $\nabla \cdot E$ and $\nabla \times E$. Therefore, the solution has to be continuous across the imagined cut.

3. Not only vanish all closed line-integrals, which they do because of $\nabla \cdot E' = 0$, but also all line integrals of E' between two corresponding points on the non-physical edges of the secondary loop vanish.

4. Similarly, all line integrals of E' between two corresponding points on the non-physical edges of the primary loop are equal to the according line integral of $\dot{A}'$.

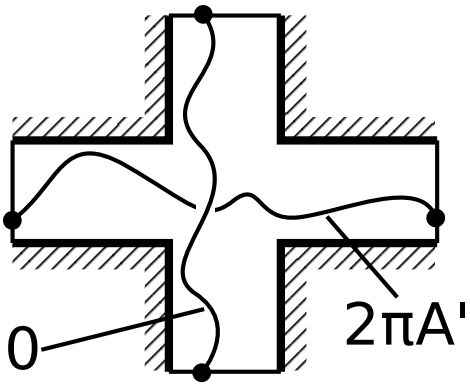

<*10*>: In order not to loose crucial information which no longer exists in two dimensions – for example the magnetic field through the primary loop – we need to impose specific conditions on the line integrals from cut to cut.

If a solution satisfying these constraints is mapped back into the original,

three-dimension domain, it will then be a solution to the original problem. Such a solution can in turn be found by means of functional analysis of complex variables, that is the theory of **holomorphic function**, for which we will have to restate the problem in the complex plane.

7. Remapping from R^2 to C

The **Cauchy-Riemann-equations** give a necessary and sufficient condition for any complex function $f:\mathbb{C}\to\mathbb{C}$ to be **complex analytic**, i.e. be holomorphic:

$$\frac{\partial \Re[f(x+\imath y)]}{\partial y}+\frac{\partial \Im[f(x+\imath y)]}{\partial x}=0$$

and

$$\frac{\partial \Re[f(x+\imath y)]}{\partial x}-\frac{\partial \Im[f(x+\imath y)]}{\partial y}=0$$

where $(\imath)^2\equiv -1$ and $\Re$ and $\Im$ denote the real and imaginary part of their argument, respectively. By nessecity, we can therefore conclude that if a complex function f, which defines two two-dimensional real functions

$$f_\xi, f_\eta : \mathbb{R}^2\to\mathbb{R}$$

by its real and imaginary part according to

$$f(z)\equiv f_\xi(\Re[z],\Im[z])-\imath f_\eta(\Re[z],\Im[z])$$

is analytic, then f_η and f_ξ constitute a vector field which is divergence-

$$\nabla\cdot\begin{bmatrix} f_\xi(x,y)\\ f_\eta(x,y)\end{bmatrix}=0$$

and curl-free:

$$\nabla\times\begin{bmatrix} f_\xi(x,y)\\ f_\eta(x,y)\end{bmatrix}=0$$

Hence, if we find a holomorphic function E_C on a domain $K_C\equiv p(K)$, the isometric image of the cross K in $\mathbb{C}$ defined by

$$p(x,y)\equiv x+\imath y+z_c$$

bijective between $\mathbb{R}^2$ and $\mathbb{C}$, then

$$E'(x,y) \equiv \begin{bmatrix} \Re[E_C(p(x,y))] \\ -\Im[E_C(p(x,y))] \end{bmatrix}$$

is a divergence- and curl-free vector field on K, i.e. a solution of the **original** differential equation. Where $z_c \in \mathbb{C}$ is chosen such, that the center of the cross lies at the origin so that the domain is twice symmetric about the real and the imaginary axis.

If, further, E_C is constrained such that the resulting E' satisfies the **boundary conditions** of the original problem, E' solves the problem completely. Because p is in a sense *one-to-one*, **isometric** everywhere under the usual metrics of $\mathbb{R}^2$ and $\mathbb{C}$, these original boundary conditions can indeed readily be translated into terms of E_C:

1. E_C^*, the complex conjugate of E_C enclose an equivalent angle γ with the physical edges of K_C. That is to say, $arg[E_C(z)]$ should be one of two opposite angles depending on the direction of the boundary at z.

2. $E_C(z) = E_C(z^*)$ and $E_C(z) = E_C(-z^*)$ for all z on the non-physical edges of K_C to permit a valid solution after transforming back to the original domain.

3. The real part of the complex integral of E_C from z to z^* has to vanish for all z on the non-physical edges of the secondary loop.

4. The real part of the complex integral of E_C from z to $-z^*$ must be equal the according real integral of A' described by the associated boundary condition on $\mathbb{R}^2$ for all z on the non-physical edges of the primary loop.

The last two conditions express the constraint that the real integral of E' take the values described in the according constraints on $\mathbb{R}^2$.

Formally, to deduce any of the constraints on $\mathbb{C}$, one performs a transformation of variables by p and takes the resulting expressions into a form which can be made sense of in $\mathbb{C}$. For example, line integrals, with x_t and y_t appropriately chosen become:

$$\begin{aligned} \int_a^b \mathrm{d}s(x,y) \cdot E'(x,y) &= \int_0^1 \mathrm{d}t \left(\frac{\mathrm{d}x_t}{\mathrm{d}t}(t)\, \Re[E_C(x_t(t) + \imath y_t(t))] - \frac{\mathrm{d}y_t}{\mathrm{d}t}(t)\, \Im[E_C(x_t(t) + \imath y_t(t))] \right) \\ &= \int_0^1 \Re[\mathrm{d}z_t]\, \Re[E_C(z_t)] - \int_0^1 \Im[\mathrm{d}z_t]\, \Im[E_C(z_t)] \end{aligned}$$

With an easy identity

$$\Re[z_0]\Re[z_1] - \Im[z_0]\Im[z_1] = \Re[z_0 z_1]$$

it follows that

$$\int_{(x_0,y_0)}^{(x_1,y_1)} \mathrm{d}s\,(x,y) \cdot E'\,(x,y) = \Re\left[\int_{p(x_0,y_0)}^{p(x_1,y_1)} \mathrm{d}z E_C(z)\right] \tag{9}$$

8. Solution of the remapped problem

Two central results of complex analysis state that the composition of two holomorphic function is again a holomorphic function and that every holomorphic function can be complex integrated to a holomorphic, **complex potential**.

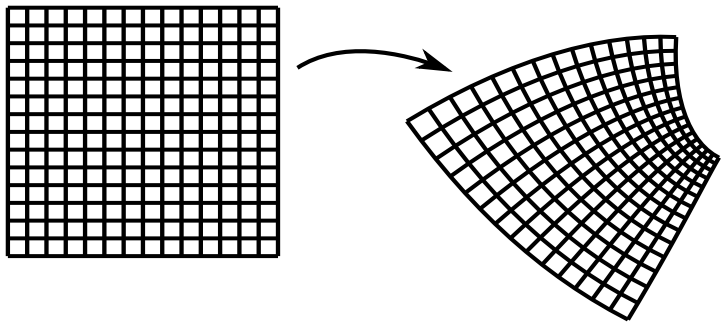

<11>: A conformal mapping preserves angles between the preimage and the image. Sometimes, it does so in an unintuitive fashion, for examples when corners are mapped onto straight lines, which is indeed possible. This picture was taken from Wikipedia's page on conformal maps.

Also, holomorphic function f is by itself **conformal**, i.e. preserving the angle at the intersection of curves $k:\mathbb{R}\to\mathbb{C}$ such that it is the same between the image of the curves, because it rotates the respective tangents along the two curves at any common point by the same angle:

$$\frac{\mathrm{d}f}{\mathrm{d}t}(k(t)) = \frac{\mathrm{d}f}{\mathrm{d}z}(z=k(t))\frac{\mathrm{d}k}{\mathrm{d}t}(t) \tag{10}$$

It is important to distinguish between the image of a **coordinate curve** under a conformal mapping f and that of a **derivative**. While f is preserving angles for to both objects individually, the derivative of a potential $U:X\subset\mathbb{C}\to\mathbb{C}$, contrary to the coordinate curve, is *covariant* with respect to f, when U is mapped onto $f(X)$:

(11)

$$\frac{\mathrm{d}U}{\mathrm{d}y}(f^{-1}(y)) = \frac{\mathrm{d}f^{-1}}{\mathrm{d}y}(y)\frac{\mathrm{d}U}{\mathrm{d}z}(z=f^{-1}(y))$$

Therefore, the derivative of a complex potential does not transform like a coordinate curve at the same point. As far as **angles** are concerned, the angle between the derivative of a potential and a coordinate curve is **not** the same as that between the derivative of the image of the potential and the image of the curve. However, if we evaluate *(11)* at $f(z)$ and complex conjugate we obtain

$$\left(\frac{\mathrm{d}U}{\mathrm{d}y}(f^{-1}(y=f(z)))\right)^* = \left(\frac{1}{\frac{\mathrm{d}f}{\mathrm{d}z}(z)}\right)^* \left(\frac{\mathrm{d}U}{\mathrm{d}z}(z)\right)^*$$

which, compared to *(10)* implies that the angle between the **complex conjucate of the derivative of the potential** U and a coordinate curve at the same point **is preserved**.

A corollary of the *Riemann-mapping theorem* further asserts that there exist **unique**, **bijective** and **holomorphic** maps between all simply-connected open true subsets of $\mathbb{C}$. The restriction that the subsets be open is only a mathematical curiosity and, by *Carathéodory's theorem* generalizes to their closure for piecewise smooth boundaries, which suffices for our purpose.

8.1. Schwarz-Christoffel-maps

Schwarz-Christoffel-maps are those (holomorphic) Riemann-maps which map from the **upper half plane** $\mathbb{H}$ to the interior of any, possibly infinite **finite-polygonial area** in $\mathbb{C}$. Whereas the Riemann-map between any two given subsets of $\mathbb{C}$ may generally be found only numerically, the form of the Schwarz-Christoffel-map $\zeta : \mathbb{H} \to \mathbb{C}$ for a given polygon is known to obey

$$\frac{\mathrm{d}\zeta}{\mathrm{d}u}(u) = s\prod_j (u-u_j)^{-\Theta_j/\pi} \qquad (12)$$

with $s \in \mathbb{C}$, $\mathrm{u}_j \in \mathbb{R}$ and $\Theta_j \in [-\pi, \pi)$, which is the *outer angle* of the polygon at each of the polygon's vertices j. Since $\mathbb{H}$ is mapped to the interior of the polygon, which is piecewise smoothly bounded, it is little surprising that the real axis $\mathbb{R}$ is mapped to the boundary of the polygon. As one may see directly from this formula, $\zeta(u_j)$ maps the **prevertex** u_j to the vertex with outer angle Θ_j because the derivative changes its direction in the complex plane when one of the exponentiated terms changes its sign.

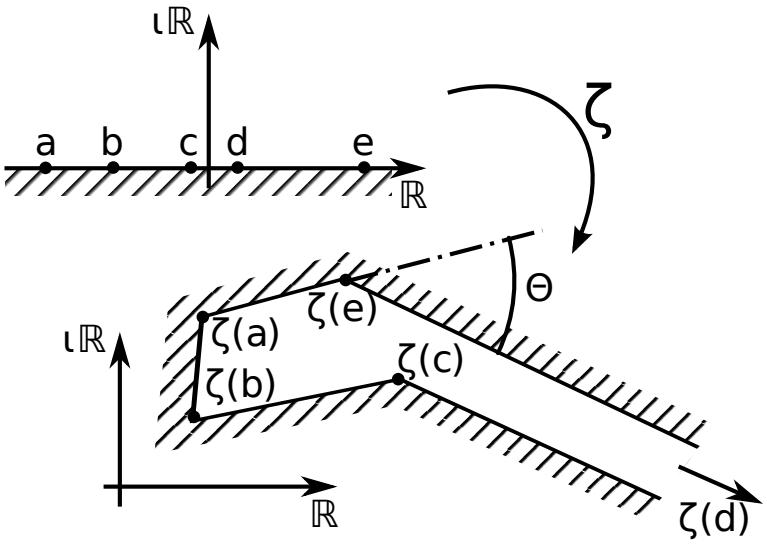

<12>: A Schwarz-Christoffel-mapping sends the upper half-plane of the complex plane onto any polygon with finitely many vertices, some of which are even allowed to sit at infinity. Its form is determined by the outer angles of the polygon. The prevertices, however, can usually only be found numerically.

Schwarz-Christoffel-maps are particularly handy to obtain approximations of practical Riemann-maps between sufficiently regular subsets because they are not as prone to numerical problems as Green's-function methods, which involve finding a kernel such as the *Szegő kernel*. An operation which exhibits “typical” numerical instability of solving differential equations whereas the a Schwarz-Christoffel-map reduces the problem to sufficiently precise **evaluation of a complex integral**. See “*Kernel functions and conformal mapping*” by S. Bergman and M. Schiffer for original work on the subject of numerically finding general Riemann-maps.

8.2. Construction of a solution

The abstract, central idea of the solution to the problem as it has been stated on $\mathbb{C}$, including boundary conditions can be described as follows:

Construct a domain $K_W \subset \mathbb{C}$ for the complex conjugate of a known holomorphic function E_W^* which makes an equivalent angle γ with parts of the boundary such that the Riemann-mapping which takes the domain to the cross K_C will map those parts onto the physical edges.

Because the Riemann-map is holomorphic, this will assure that the image E_C of the **known** holomorphic function, the sought solution, is a holomorphic function in turn. Further, using the result following *(10)* and *(11)*, with the boundary of K_W being the coordinate curve, E_C^* will make the

desired angle γ with the boundary of K_C and thus satisfy the first boundary condition.

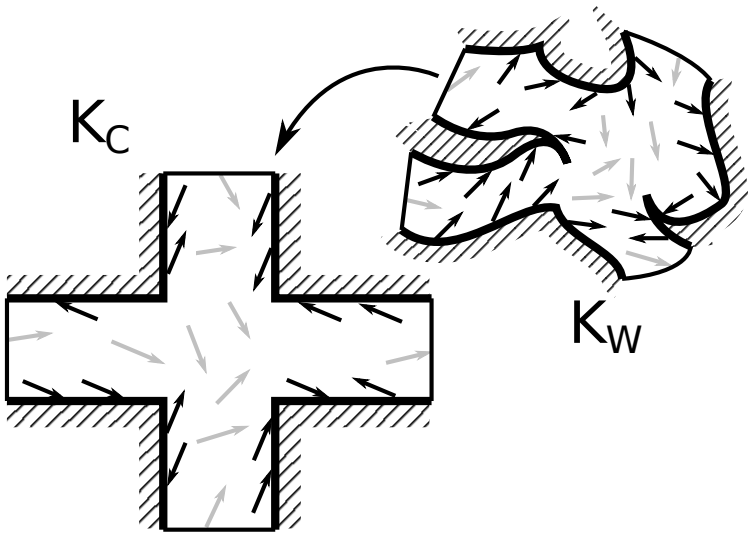

<13>: The general idea is to build a domain which encloses the Hall angle with some holomorphic electric field and transform this back onto the cross.

It can be shown that **if** a solution E_C to the complete problem exists at all, which is non-vanishing almost everywhere – practically everywhere –, then this construction with any arbitrarily chosen non-vanishing E_W permits to find it, although the additional constraints are not a-priori satisfied and need to be considered in details of the construction.

Because E_C and E_W are holomorphic, they can both be integrated to a respective **complex potential** U_C and U_W. U_C is, by the inverse function theorem **biholomorphic** and can be taken into U_W by a conformal map $W_C^{-1} \equiv U_C^{-1} \circ U_W$ so that

$$U_C \circ W_C^{-1} : K_W \to \mathbb{C}$$

where W_C^{-1} preserves the angle between E_C^* and ∂K_C to E_W^* and ∂K_W. Therefore, the solution lies in the space of solutions allowed for by the above construction and the boundary conditions, if they can be satisfied, can still be accounted for within that space.

8.2.1. Details of the construction process

To begin with, we make the simplest possible choice for the preimage $E_W : K_W \to \mathbb{C}$, namely $E_W \equiv 1$, which implies $E_W^* = E_W$, so that the preimage of the physical boundaries actually make a an equivalent angle γ with the real axis of K_W. The according **complex potential**, which is the recipient of W_C so becomes

(13)

$$U_W(z) = z$$

By construction, E_C will then automatically satisfy the differential equation, i.e. be holomorphic and the first boundary conditions. The remaining boundary conditions can then be satisfied by using the available degrees of freedom.

Specifically, we will exploit those freedoms directly in the construction of K_W only to satisfy the **second** constraint, that is that the field transit smoothly across the non-physical edges. The class of solutions obtained thus far will satisfy the first and the second constraint and have a **constant** line integral between all corresponding points on the non-physical edges of the primary and the secondary loop, each.

Solutions can eventually be superposed as a **linear combination** on the original problem domain – corresponding to using yet another freedom on K_W – to satisfy the last two constraints. Such a combination retains accordance with the first two constraints and the final solution to the complete problem is obtained.

8.2.2. Approximation on the preimage of the domain

From how we have chosen E_W, the preimage of E in the W-plane, we can immediately infer that the preimage of the coordinate curve parametrizing ∂K_E has to go along an angle of γ with respect to the real axis, either *forwards* or *backwards*, which attributes to the fact that there are two possible equivalent angles.

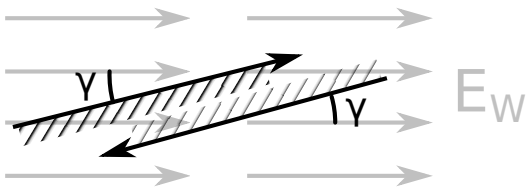

<14>: The boundaries of K_W which correspond to the physical boundaries of the conductor may go along either two opposing directions.

The **freedom**, so to speak, is then reflected in the choice between "*forwards*" and "*backwards*" at any point of ∂K_W and the ambivalence of how the **non-physical** boundaries are mapped. However, in order to use Schwarz-Christoffel-maps, we restrict ourselves to finite-polygonial K_W, meaning the preimage of the non-physical boundaries is taken to be piecewise straight. Because we know that an appropriately chosen K_W will yield the correct solution E_C and our question for K_W is thus well-posed, we can regard this limitation as **approximating** the correct K_W, the non-physical boundary of which is actually smooth (as will be illustrated).

For practical simplicity, we even go as far as not only approximating the non-physical boundary piecewise polygonially, but rather as just a **single straight line** in the actual implementation. Despite this seemingly rough a-priori restriction, the solution will turn out completely satisfactory.

8.3. Cconformal map between K_W and K_C

Any Schwarz-Christoffel-mapping yields a **biholomorphic** map between $\bar{\mathbb{H}} \equiv \mathbb{H} \cup \mathbb{R}$ and the target domain. A **Möbius-transform** may biholomorphically map $\bar{\mathbb{H}}$ to the closure of the unit disk $\bar{\mathbb{D}} \subset \mathbb{C}$. Under the assumptions made above, we can therefore obtain a biholomorphic map between K_C and K_W via either $\bar{\mathbb{D}}$ or $\bar{\mathbb{H}}$.

First, we will transform the Christoffel-Schwarz-map into a map $C : \bar{\mathbb{D}} \to K_C$, which turns out to have the exact same form like *(12)* with the prevertices accordingly mapped onto the unit disk by a Möbius-transform. It should be intuitively clear that C is much less distorted than the original Schwarz-Christoffel map and therefore better suited for numerical evaluation.

We will then derive relations between the prevertices which follow directly from **symmetry** of K_C so that we are left with only **four unknowns** which correspond to the four geometrical degrees of freedom of the cross K_C.

Finally, $W^+ : \bar{\mathbb{D}} \to K_W^+$ and $W^- : \bar{\mathbb{D}} \to K_W^-$ are derived, which map the physical edges onto appropriately aligned edges each, with an additional freedom for the non-physical edges, which we will use to achieve a smooth transition thereover. The superscripts "$+$" and "$-$" are called so according to the sign of the resulting line integral along the secondary loop. According to *(13)*

$$U_C^+(z) \equiv U_W(W_C^+(z)) \equiv (W^+ \circ C^{-1})(z)$$

and

$$U_C^-(z) \equiv U_W(W_C^-(z)) \equiv (W^- \circ C^{-1})(z)$$

will be potentials yielding E_C^+ and E_C^- in the C-plane, which can be scaled and linearly combined as

$$E_C \equiv \alpha_+ E_C^+ + \alpha_- E_C^-$$

with $\alpha_+, \alpha_- \in \mathbb{R}$ to cancel out the line integral along the secondary loop match the desired value along the primary loop.

8.3.1. Transformation of the Schwarz-Christoffel-mapping

The **Caley transform**, a specific form of Möbius-transformation, bijectively maps $g : \bar{\mathbb{H}} \to \bar{\mathbb{D}}$. Inserting

$$g^{-1}(z) \equiv \imath \frac{1+z}{1-z}$$

into a Schwarz-Christoffel-map to K

$$\zeta(z) = \zeta_0 + s \int_0^z \mathrm{d}y \prod_j (y - u_j)^{-\Theta_j/\pi}$$

therefore yields a biholomorphic map $\zeta \circ g^{-1} : \bar{\mathbb{D}} \to K$ which can be taken into a nicer form by transformation of the integral

$$\begin{aligned}
\zeta(g^{-1}(z)) &= \zeta_0 + 2\imath s \int_\imath^z \mathrm{d}y \frac{1}{(1-y)^2} \prod_j \left(\imath \frac{1+y}{1-y} - u_j \right)^{-\Theta_j/\pi} \\
&= \zeta_0 + 2\imath s \int_\imath^z \prod_j (\imath(1+y) - u_j(1-y))^{-\Theta_j/\pi} \\
&= \zeta_0 + 2\imath \prod_j (\imath + u_j)\, s \int_\imath^z \prod_j \left(y - \frac{u_j - \imath}{u_j + \imath} \right)^{-\Theta_j/\pi} \\
&= \zeta_0 + 2\imath \prod_j (\imath + u_j)\, s \int_\imath^z \prod_j (y - g(u_j))^{-\Theta_j/\pi}
\end{aligned}$$

where we used the fact that the sum of all outer angles Θ_j of a polygon adds up to 2π so that the rescale of the measure could be dissolved in the product. Therefore, the newly obtained map has the exact same form like *(12)* with the **integrand remapped** onto $\bar{\mathbb{D}}$, the new vertices on the boundary of $\mathbb{D}$. In fact, both mappings are commonly referred to as Schwarz-Christoffel-mappings.

It must be noted with great care that the branch of the (generally real) power in the integrand of the Schwarz-Christoffel mapping ought to be chosen consistently to how it arises from the terms $(z - u_j)^{-\Theta/\pi}$. In these

terms, the branch is naturally chosen such that the result is continuous in z. While this consideration is superflous in the traditional form of the Schwarz-Christoffel-map where the **principal branch** is continous for z, which has $-\pi \leq arg\,[z-u_j] \leq \pi$, it needs to be specifically considered for $z \in \bar{\mathbb{D}}$ because the principal branch is no longer continous for arbitrary polar angles of $z-u_j$. In practice, the following evaluation rule makes the power continous for all z with $|z| \leq 1$, $r \in \mathbb{R}$

$$(z-u_j)^r \equiv e^{r\imath\left(arg\,[u_j]+\frac{\pi}{2}\right)} exp\left(rln\left((z-u_j)\,e^{\imath\left(-arg\,[u_j]-\frac{\pi}{2}\right)}\right)\right)$$

where the logarithm is taken on its principal branch.

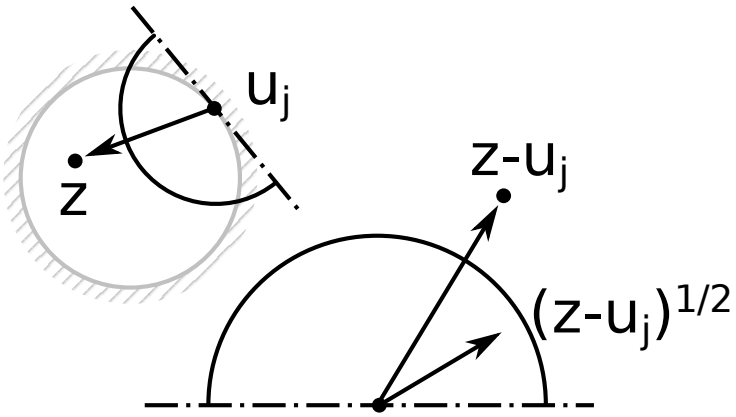

<15>: The evaluation rule for the power relies on the fact that the principal branch is continuous for a sector of π. After using the principal branch for evaluation, the result is transformed back, which makes the overall operation continuous.

8.3.2. Symmetry relations

Because of the specific form of K_C, among other things symmetric about the real and the imaginary axis, it is fully parametrized by three (real) parameters determining the shape plus two additional (complex) ones, determining the overall scale, rotation and position. Conversely, C has only five parameters, three of them being the prevertices, one being the scale $s_C \in \mathbb{C}$ and the last one being the integration constant.

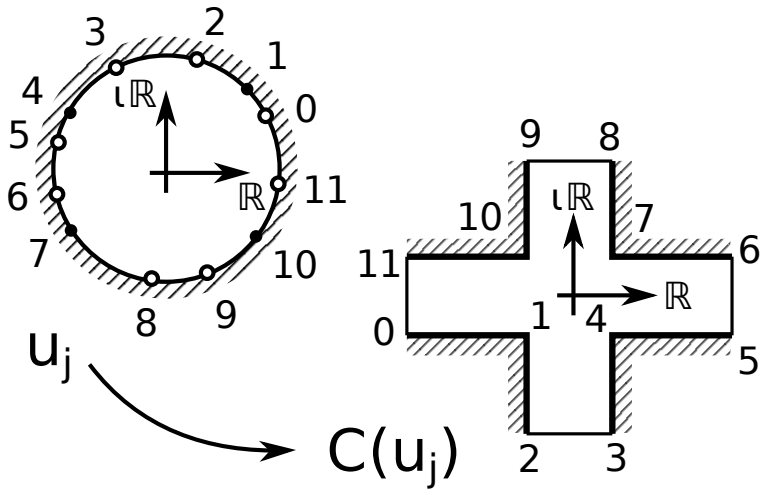

<16>: The map C from the unit disk onto the cross. The position of the prevertices u_j still has to be determined and is ultimately related to the specific geometry of the cross.

If we choose the lower end of the integral to be 0 and require that $0 \in \mathbb{D}$, the center of the unit disk map to $0 \in K_C$ this fixes the integration constant to 0 and leaves us with

$$C(u) = s_C \int_0^u \mathrm{d}y \left(\frac{(y-u_1)\,(y-u_4)\,(y-u_7)\,(y-u_{10})}{(y-u_0)\,(y-u_2)\,(y-u_3)\,(y-u_5)\,(y-u_6)\,(y-u_8)\,(y-u_9)\,(y-u_{11})} \right)^{1/2}$$

which maps the **counter-clockwise** u_j onto the **counter clockwise** boundary of K_C. The complex conjugate is **anti-holomorphic** which permits the following transformation

$$\begin{aligned} C(u^*) &= s_C \int_0^{u^*} \mathrm{d}y \prod_j (y-u_j)^{-\Theta_j/\pi} \\ &= s_C \int_0^{u} (\mathrm{d}y)^* \prod_j (y^*-u_j)^{-\Theta_j/\pi} \\ &= s_C \int_0^{u} (\mathrm{d}y)^* \Big(\prod_j (y-u_j^*)^{-\Theta_j/\pi} \Big)^* \\ &= s_C \left(\int_0^{u} \mathrm{d}y \prod_j (y-u_j^*)^{-\Theta_j/\pi} \right)^* \end{aligned} \qquad (14)$$

Therefore, $C(u^*)$ maps the **counter-clockwise** unit circle **clockwise** onto ∂K_C. We may always assume $s_C \in \mathbb{R}$ without loss of generality because if it was not, a rotary transform could make it so. Then

$$C^*(u^*) = s_C \int_0^{u} \mathrm{d}y \prod_j (y-u_j^*)^{-\Theta_j/\pi}$$

maps the counter-clockwise unit circle **counter-clockwise** onto $\partial K_C^* = \partial K_C$ because of symmetry.

Because this is again a Schwarz-Christoffel-map which is **unique**, given a fixed point – in this case the origin – and rotation – the argument of s_C – we can conclude that $C(u)$ and $C^*(u^*)$ are in fact the same map and have the same distribution of prevertices around the unit circle. Hence, the u_j must be symmetric about the real axis

$$u_j = u^*_{11-j}$$

and, subsequently

$$C(u^*) = C^*(u) \tag{15}$$

An analogous argument can be constructed for symmetry about the imaginary axis by using $-u^*$ producing

$$C(-u^*) = -C^*(u) \tag{16}$$

Eventually, we obtain full symmetry for all of the domain, leaving three u_j undetermined so that

$$C(u) = s_C \int_0^u \mathrm{d}y \left(\frac{(y^2 - u_1^2)\,(y^2 - (u_1^*)^2)}{(y^2 - u_0^2)\,(y^2 - (u_0^*)^2)\,(y^2 - u_2^2)\,(y^2 - (u_2^*)^2)} \right)^{1/2} \tag{17}$$

with u_0, u_1, u_2 counter clockwise in the first quadrant of the unit circle, depending on the **ratios of the geometry**.

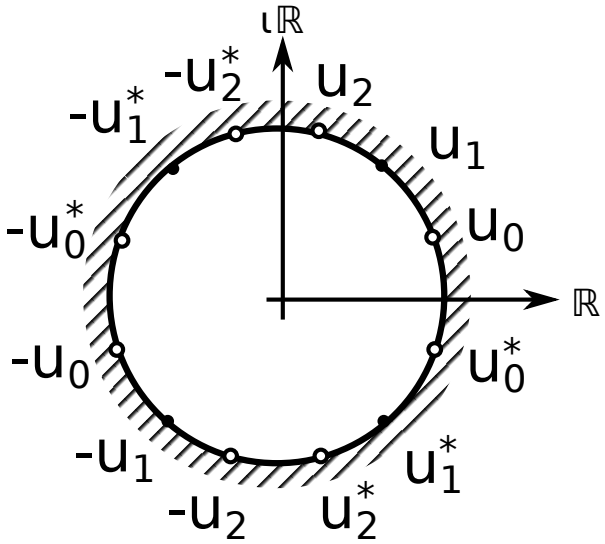

<17>: The prevertices are as symmetric as the domain to which they map. With a bit of imagination, one may see how the position of the prevertices along the circle relates to the ratios of geometry.

As a rule of thumb, the ratios of the distances between the corresponding vertices somewhat resemble those between the corresponding prevertices.

8.3.3. Mappings from the unit disk to K_W

We construct two different K_W, namely K_W^+ and K_W^-, each of which has appropriately chosen edges to satisfy the first boundary condition, satisfy the second boundary condition approximately and have a constant potential difference between the according non-physical edges, each.

Because we know that C maps the arcs between the respective u_j onto the edges of K_C, we can construct K_W by a Schwarz-Christoffel-Transform W with the same prevertices and fix the angles Θ_j between the images of the edges to our liking. Eventually, $W \circ C^{-1}$ will then map edges of K_C to differently related edges of K_W and we can choose a suitable rotation s_W to achieve the desired angle between E_W and the ∂K_W.

$$W^+(u) \equiv s_W^+ \int_0^u \mathrm{d}y \frac{y^2 - u_1^2}{(y^2-u_0^2)^{1/2-\beta}\,(y^2-u_2^2)^{1/2-\alpha}\,(y^2-(u_0^*)^2)^{1/2+\beta}\,(y^2-(u_2^*)^2)^{1/2+\alpha}}$$

with $\alpha, \beta \in (-1/2, 1/2)$ two **free parameters** which allow us to approximate a smooth transition across the non-physical edges of the primary (β) and the secondary (α) loop while maintaining the necessary angle of the physical edges.

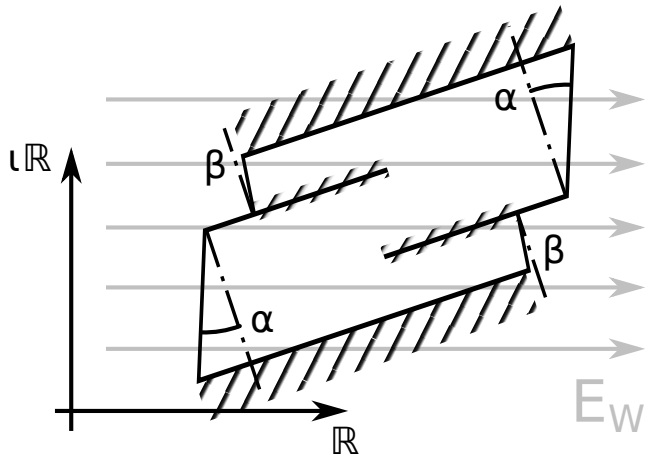

<18>: The W, in this case W^+, maps the cross to a shape where the top arm is bent onto the left arm and the bottom arm bent onto the right. W^- does the opposite and looks pretty much the same, just reflected.

α and β are determined by a two dimensional optimization problem minimizing the deviation of E_C. In the following, we shall declare $v \doteq C^{-1}(z)$ so that

(18)

$$E_C(z) \equiv \frac{\mathrm{d}U_C}{\mathrm{d}z}(z) = \frac{\frac{\mathrm{d}W}{\mathrm{d}v}(v)}{\frac{\mathrm{d}C}{\mathrm{d}v}(v)}$$

and the optimization problem becomes

$$\min_{\alpha,\beta}\left[\int_{C(u_2)}^{C(u_3)}\mathrm{d}z|E_C(z) - E_C(z^*)| - \iota\int_{C(u_5)}^{C(u_6)}\mathrm{d}z|E_C(z) - E_C(-z^*)|\right] \qquad (19)$$

where the integral is to be understood as a curve integral along the according non-physical edges.

Let us consider the expression for E_C at different values of v, specifically $v = u_j$. Numerator and denominator in *(18)* are both known **analytically**. Only for points other than the vertices we need to calculate the preimage $v \in \mathbb{D}$ to obtain a value for E_C. Comparing the powers in the respective derivatives, we note that every $\alpha \neq 0$ or $\beta \neq 0$ will cause **singularities** and **zeroes** of order less than $1/2$ at the according vertices, because the singularities in the derivatives of C and W no longer cancel eachother. To make things worse, the same vertex on a pair of non-physical edges, for example u_j and u_j^*, gets one singularity and one zero, as α or β change away from 0. Making E_C match perfectly is therefore impossible, unless it is already matching with $\alpha = \beta = 0$.

This is characteristic of holomorphic maps, especially Schwarz-Christoffel-maps and vividly illustrates the seemingly unintuitive property that we map a corner of a certain angle – $\pi/2$ in K_C – onto a corner of a arbitrary angle while **preserving angles** between coordinate curves. If the latter angle is unequal the first, this leads to singular behaviour, eluding our intuition.

The exact solution obviously has no such issues. But as we have shown, the exact solution lies in our theoretical space of solutions and may therefore be obtained by an appropriate Riemann-mapping. Such a mapping would have a similarly aligned image of the physical boundaries while the image of the non-physical boundaries could perfectly satisfy continuity across the non-physical edges. The only way this can happen is if the necessary bending along the image of non-physical edges is achieved smoothly, with “infinitesimal distortions”, the mathematical description of which is beyond the scope of this report.

The line integrals in *(19)* can be pulled back onto the unit circle to evade calculating v and simplified by using

$$\frac{\mathrm{d}C}{\mathrm{d}u}(u = -v^*) = \frac{\mathrm{d}C}{\mathrm{d}u}(u = v^*) = \left(\frac{\mathrm{d}C}{\mathrm{d}v}(v)\right)^*$$

We know that K_W is constructed such that E_C has a consistent angle at the same point on two respective non-physical edges. By virtue of *(18)* the expression then becomes

$$\left[\int_{u_2}^{u_3} \mathrm{d}u \frac{\mathrm{d}C}{\mathrm{d}u}(u) \, || E_C(C(u)) | - | E_C(C(u^*)) || - \iota \int_{u_5}^{u_6} \mathrm{d}u \frac{\mathrm{d}C}{\mathrm{d}u}(u) \, || E_C(C(u)) | - | E_C(C(-u^*)) || \right.$$

$$= \min_{\alpha,\beta} \left[\int_{arg[u_2]}^{arg[u_3]} \mathrm{d}\varphi \, || \frac{\mathrm{d}W}{\mathrm{d}u}(u = e^{\iota\varphi}) | - | \frac{\mathrm{d}W}{\mathrm{d}u}(u = e^{-\iota\varphi}) || + \int_{arg[u_5]}^{arg[u_6]} \mathrm{d}\varphi \, || \frac{\mathrm{d}W}{\mathrm{d}u}(u = e^{\iota\varphi}) | - | \frac{\mathrm{d}W}{\mathrm{du}}(u = e^{-\iota\varphi + \pi}) || \right.$$

The integral is evaluated numerically along the arcs and the minimum is attained at α and β smaller than 0, which "relaxes" the distortion of W_C along the non-physical edges.

W^- is constructed much like W^+, but instead of bending the arms of the secondary loop clockwise, they are bent counter-clockwise, so that the resulting E_C^* goes against the imaginary axis.

$$W^-(u) \equiv s_W^- \int_0^u \mathrm{d}y \frac{y^2 - (u_1^*)^2}{(y^2 - u_0^2)^{1/2+\beta} (y^2 - u_2^2)^{1/2+\alpha} (y^2 - (u_0^*)^2)^{1/2-\beta} (y^2 - (u_2^*)^2)^{1/2-\alpha}}$$

with α and β being those angles which we obtained from minimizing *(19)*. Correctness with respect to our requirements can easily be asserted by noting that

$$\frac{1}{s_W^-} \frac{\mathrm{d}W^-}{\mathrm{d}v}(v = u^*) = \left(\frac{1}{s_W^+} \frac{\mathrm{d}W^+}{\mathrm{d}u}(u) \right)^* \qquad (20)$$

which leaves the minimization problem forminvariant, so that the derivation is equally valid for finding the desired W^-. Finally, we require $|s_W^+| = |s_W^-| = 1$ without loss of generality because we later linearly combine E_C^+ and E_C^- with two **real coefficients**, anyway. By construction, we know that s_W^+ and s_W^- rotate the preimage of edge 0 to go along the Hall angle γ for W^+ and W^-, respectively. This determines the argument of s_W^+ for numerical implementation with u_s anywhere on the arc between u_0 and u_1

$$arg\left[\frac{\mathrm{d}W^+}{\mathrm{d}u}(u = u_s) \right] + arg[u_s] + \frac{\pi}{2} \equiv \gamma$$

Consequently, u_s^* lies on the arc betwen u_{10} and u_{11}, which leads to a similar condition for s_W^-:

$$arg\left[\frac{\mathrm{d}W^{-}}{\mathrm{d}u}(u=u_s^*)\right]+arg\,[u_s^*]+\frac{\pi}{2}\equiv\gamma+\pi$$

By *(20)* and $arg\,[u^*]=-arg\,[u]$, there is thus a fixed relation between s_W^+ and s_W^-

$$s_W^+ s_W^- = exp\,(\imath 2\gamma) \tag{21}$$

With an anti-holomorphic integral transform much like *(14)* we can therefore infer full symmetry between the image of K_W^+ and K_W^-. Latter is obtained from the former and vice versa by **reflection about the axis along the Hall angle** γ:

$$\frac{W^-(u^*)}{s_W^-}=\left(\frac{W^+(u)}{s_W^+}\right)^* \tag{22}$$

8.3.4. Linear combination into the final solution

The **potential difference** between two corresponding points on the respective, non-physical edges is defined in terms of E_C and, by *(9)* in K_W becomes the real distance between the two preimage points:

$$\Re\left[\int_a^b \mathrm{d}z E_C(z)\right]=\Re\left[\int_{C^{-1}(a)}^{C^{-1}(b)}\mathrm{d}u\frac{\mathrm{d}W}{\mathrm{d}u}(u)\right]=\Re[W_C(b)-W_C(a)]$$

By how we have fixed the angles of W, the preimages of the non-physical edges at which the potential is evaluated are parallel as by point symmetry of W

$$W(-u)=-W(u) \tag{23}$$

The potential difference between the eight corresponding vertices of the non-physical edges is therefore the same for each loop. However, following *(19)* we have established that the bordering E_C is only approximately consistent at the non-physical edges in K_C. Writing the potential difference between two corresponding points on the non-physical edges of the secondary loop z and z^* as

$$\Re\left[\int_z^{z^*}\mathrm{d}z E_C(z)\right]=\Re[W(u_8)-W(u_3)]+\Re\left[\int_z^{z^3}\mathrm{d}y\left(E_C(y)-E_C(y^*)\right)\right]$$

suggests that only if the minimization problem is solved to 0, meaning perfectly consistent fields across the non-physical edges, the potential difference is constant. The same reasoning applies to the primary loop.

We base the linear combination upon the values taken on at the vertices, so that the sought coefficients are determined by

$$\alpha_+ \mathcal{R}[\,W^+(u_5) - W^+(u_0)\,] + \alpha_- \mathcal{R}[\,W^-(u_5) - W^-(u_0)\,] = 2\pi R A' = \pi R^2 b_0$$

for the primary loop and

$$\alpha_+ \mathcal{R}[\,W^+(u_9) - W^+(u_2)\,] + \alpha_- \mathcal{R}[\,W^-(u_9) - W^-(u_2)\,] = 0$$

for the secondary loop. From the **symmetry** relations of K_W^+, K_W^- and the associated maps, we can directly deduce relations between the potential difference. Regarding the **potential across the secondary loop**, from *(22)* and $|s_W^+| = 1$ we have that

$$\begin{aligned} e^{\imath\gamma}\Delta_2 \equiv W^+(u_9) - W^+(u_2) &= W^+(u_2^*) - W^+(u_9^*) \\ &= -s_W^- s_W^+ (\,W^-(u_9) - W^-(u_2)\,)^* \end{aligned}$$

With *(21)* the ratio between α_- and α_+ can be obtained:

$$\frac{\alpha_+}{\alpha_-} = \frac{\mathcal{R}\left[e^{\imath\gamma}\Delta_2^*\right]}{\mathcal{R}[e^{\imath\gamma}\Delta_2]}$$

The same argumentation leads to an expression from the condition across the primary loop, by virtue of *(23)* with a positive sign

$$\alpha_+ \mathcal{R}[e^{\imath\gamma}\Delta_1] + \alpha_- \mathcal{R}\left[e^{\imath\gamma}\Delta_1^*\right] = \pi R^2 b_0$$

where $e^{\imath\gamma}\Delta_1 \equiv W^+(u_5) - W^+(u_0)$ accordingly. Both, Δ_1 and Δ_2 depend only on the geometry of K_C and do not depend on γ. After a bit of rearranging the terms, we arrive at expressions for α_+ and α_- in terms of the Hall angle γ for a given geometry

$$\alpha_+ = \pi R^2 b_0 \frac{cos\gamma + m_0 sin\gamma}{m_1 sin^2\gamma - m_2 cos^2\gamma}$$

and

$$\alpha_- = \pi R^2 b_0 \frac{cos\gamma - m_0 sin\gamma}{m_1 sin^2\gamma - m_2 cos^2\gamma}$$

with m_0 through m_2 geometry constants defined as

$$\begin{aligned} m_0 &\equiv \frac{1}{tan\,arg\,[\Delta_2]} \\ m_1 &\equiv -2\,|\Delta_1|\,tan\,(arg\,[\Delta_2]\,)\,sin\,(arg\,[\Delta_1]\,) \\ m_2 &\equiv -2\,|\Delta_1|\,cos\,(arg\,[\Delta_1]\,) \end{aligned}$$

Note that because of $arg\,[\Delta_1] < 0 < arg\,[\Delta_2]$ neither of the coefficients has any poles. This property will be important when we consider properties of the solution, where the same denominator will appear again.

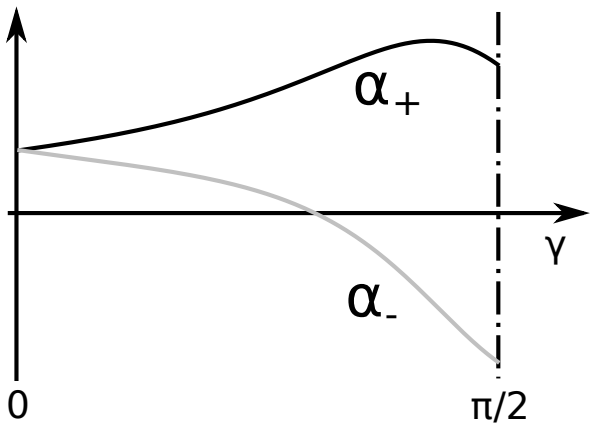

<19>: The characteristic behaviour of the coefficients for the superposed solutions the potential of which across the secondary loop is to compensate.

8.4. Properties of the solution

Because the solution is, although approximate, analytic but with respect to constants which depend only on the ratios of geometry of the original domain, various properties can be obtained. A few of them we derive here.

From *(4)* we know that the **current** is related to the electric field by a rotation and scale by a constant. The current

$$j_C(z) \equiv j_x(\Re[z], \Im[z]) + \imath j_y(\Re[z], \Im[z])$$

in the complex plane can thus be expressed in terms of E_C by

$$j_C(z) = \sigma E_C^*(z)$$

where $\sigma \in \mathbb{C}$ is the complex conductivity with $arg[\sigma] = \gamma$ rotating the current such, that it is parallel to the boundary. With

$$\Re[z_0]\Im[z_1] - \Im[z_0]\Re[z_1] = -\Im[z_0 z_1^*]$$

the **flux** I of j through a curve k in $\mathbb{R}^2$ can be written as a complex integral over the corresponding curve in K_C:

$$\begin{aligned} I &= \int_k \mathrm{d}s(x,y) \times j(x,y) \\ &= \Im\left[\int_{p(k)} \mathrm{d}z j_C^*\right] \\ &= \Im[\sigma^* \int_{p(k)} \mathrm{d}z E_C(z)] \end{aligned} \qquad (24)$$

8.4.1. External conductivity

The ratio of the current through the primary loop I_1 over the induced voltage $\pi R^2 b_0$ is interesting because without a magnetic field it corresponds to the overall loss in the conductor. From *(24)* we can proceed analogously to how the coefficients α_+ and α_- were calculated to obtain

$$I_1 = |\sigma| \Im[\Delta_3] (\alpha_+ + \alpha_-) = 2\pi R^2 b_0 |\sigma| \Im[\Delta_3] \frac{cos\gamma}{m_1 sin^2\gamma - m_2 cos^2\gamma}$$

with $e^{\imath\gamma}\Delta_3 \equiv W^+(u_6) - W^+(u_5)$ a geometry constant and the argument of σ cancels against the according exponential term from *(22)*. Apparently, I_1 vanishes for $\gamma = \pi/2$, as one would have guessed.

8.4.2. Hall effectiveness

Similarly, an expression for the flux through the secondary loop I_2 can be derived. This time, a negative sign between the coefficients α_1 and α_2 so that with $e^{\imath\gamma}\Delta_4 \equiv W^+(u_3) - W^+(u_2)$:

$$I_2 = 2\pi R^2 b_0 |\sigma| \Im[\Delta_4] \frac{2m_0 sin\gamma}{m_1 sin^2\gamma - m_2 cos^2\gamma}$$

Put together, we have the ration between the current that we “put into” the primary loop and that which results in the secondary loop

$$\frac{I_2}{I_1} = m_0 \frac{\Im[\Delta_4]}{\Im[\Delta_3]} tan\gamma$$

which agrees with our expectation that in the limit of a Hall angle of 90 degrees, the current circulates only in the secondary loop.

9. Implementation

Sage – William A. Stein et al. Sage Mathmematics Software (Version 5.10), The Sage Development Team, 2013, http://www.sagemath.org – an open, unified mathematics enviroment which, in turn, interfaces to other open software such as Maxima – *http://maxima.sourceforge.net. Maxima, a Computer Algebra System* – is used in aid to this work, such as for symbolics and simplifications. Eventually, it is aso used to implement the solution so that specification of the constraints (geometry, potential difference across the primary loop, etc.) will yield a complete solution, i.e. the electric field and resulting current on K_C.

The program code is written in the *Python Programming Language* and substructured into a module which calculates Schwarz-Christoffel-maps and their inverse, a module which renders related plots and the main code,

which is given

- the ratio between the breadth and the length of the primary loop,
- the ratio between the breadth and the length of the secondary loop,
- the ratio between the breadth of the secondary loop and that of the primary loop,
- the desired potential across the primary loop, and
- the Hall angle and conductivity $|\sigma| = 1/\sqrt{R^2 + (B/\rho)^2}$ of the conductor.

Schwarz-Christoffel-maps are accordingly evaluated on the unit disk. The according integrator can be given any two points on the unit disk and returns the integral. For stability, the contour of the integral is chosen piecewise straight such that it “snaps” to the prevertices on the boundary if any segment would get closer to it than a specific tolerance. Unless two prevertices are as close together as for their tolerances to overlap, the contour is then piecewise ending at any vertex which it is close at. The resulting contour is then piecewise evaluated using **Gauss-Jacobi-Quadrature** for the pieces at the prevertices and a generic integrator for the rest.

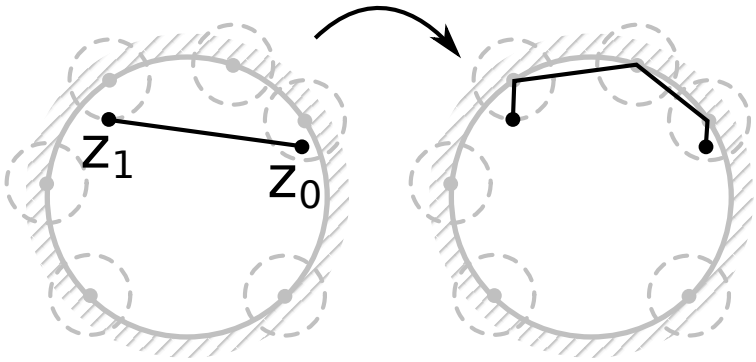

<20>: The algorithm which calculates a contour integral within the unit disk snaps the contour to the poles, so that Gauss-Jacobi-Quadrature can be used to stabilize the evaluation.

The **inverse** of the Schwarz-Christoffel-map is found basically using a **Newton iteration**, because the analytic expression for the derivative of the map is available as by *(12)*. The inverse is **cached** in a set of rectangular, two-dimensional arrays, tailored to the shape of K_C. As a side-effect, each testwise iteration of the inversion yields a value which can

possibly be fed into the cache, to minimize the amount of redundant integral evaluations.

9.1. Results of the implementation

Once the Schwarz-Christoffel-map C and its inverse C^{-1} are calculated for a given geometry, the electric field and thus current for **any** point follow directly and analytically as by *(18)*. Therefore, the electric field in a given geometry for any Hall angle can be calcuated with just a few dozen arithmetic evalations. Further, stability of the result is generally good and determined only by the quality of the inverse and **independent** of the Hall angle.

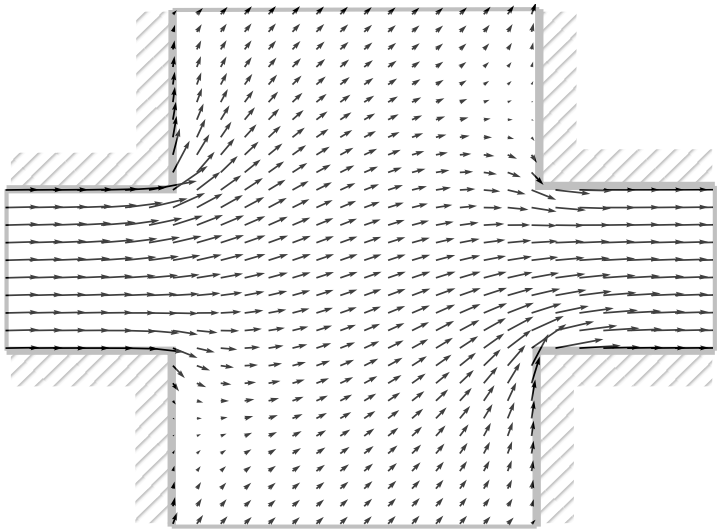

<21>: Example of a solution for a not fully symmetric geometry with Hall angle 35°. The arrows indicate the direction of the current. The effect of the approximation can be seen by inconsistent magnitude of the the current near the corners of the non-physical edges, as they approach the artificial singularities.

All properties of the solution which do **not** refer to a point in K_C **other than** the vertices can be expressed analytically on the unit disk. For example, the **energy loss** can be calculated:

Thinking back to *(1)*, there occurs a *drag* or *friction* term acting on the continuum of mobile charge carriers. Multiplying with the velocity j/ρ should yield a dissipation power per unit area:

$$P_d = j^2 R$$

which we recognize as the **Joule heat**. Integrated over all of K, this will give us the overall dissipation. For that, let us express j in terms of j_C

which in turn follows from E_C by multiplication with σ. We then have

$$P_d = R\sigma^2 \int_{K_C} \mathrm{d}x\mathrm{d}y \left(\Re[E_C(x+\imath y)]^2 + \Im[E_C(x+\imath C)]^2 \right)$$

The coefficient conveniently reduces to $R\sigma^2 = cos\gamma$. This real $\mathbb{R}^2$ integral can be transformed onto the unit disk in $\mathbb{R}^2$ by using the complex transform C as a real transform like

$$\begin{bmatrix} x \\ y \end{bmatrix} = \begin{bmatrix} \Re[C(u+\imath v)] \\ \Im[C(u+\imath v)] \end{bmatrix}$$

which, by virtue of holomorphy of C, makes this effectively a pull-back onto the (real) unit disk as

$$\begin{aligned} P_d &= cos\gamma \int_{\{r \in \mathbb{R}^2 \,|\, |r| \leq 1\}} \mathrm{d}u\mathrm{d}v \left| \frac{\mathrm{d}C}{\mathrm{d}z}(z = u+\imath v) \right|^2 \left| \alpha_+ E_C^+(u+\imath v) + \alpha_- E_C^-(x+\imath y) \right|^2 \\ &= cos\gamma \int_{\{r \in \mathbb{R}^2 \,|\, |r| \leq 1\}} \mathrm{d}u\mathrm{d}v \left| \alpha_+ W^+(u+\imath v) + \alpha_- W^-(x+\imath y) \right|^2 \end{aligned}$$

The integrand in this expression has a poles of order greater than $1/2$ at all those prevertices which delimit non-physical boundaries. Therefore, and because of the approximation we made, it is not integrable towards the corners of the non-physical edges. Since we know that the exact solution would **not** have any such poles and further, because we know that our solution is a good approximation we can conclude that the wrong behaviour is actually restricted to the proximity of these corners. In order to perform the integral, one may therefore construct an *ad-hoc* correction for the integrand.

In the implementation, the correction was chosen such that as the integral gets close to the problematic corner, the point of evaluation “stagnates” towards a point which is ε towards the center of the unit disk. This effectively makes the electric field on K_C at the corners take a value a bit away from the corners.

It might be interesting to know how the electric field behaves along the secondary loop for the potential to vanish **although** there is a current flowing along that loop. As can be shown, the according potential varies antisymetrical as a sine along the symmetry axis in the secondary loop. Along the increasing flank, the magnetic force pushes against the electric field and provides the required energey for the overall integral to vanish. For different loops which do not coincide with the symmetry axis, the potential has to be evaluated numerically and becomes a strongly distorted sine.

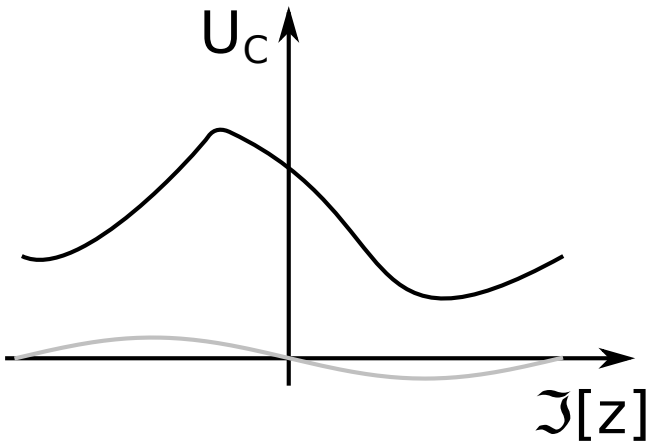

<*22*>: The characteristic behaviour of the potential along the secondary loop. In gray the potential along the symmetry line. In black the potential quarter of the breadth in from the boundary.

10. Further considerations

Besides the obvious, calculating an **exact** solution, **uniqueness** and **existence** of the solution is a question not conclusively answered by this report. The way how the K_W are constructed suggests that the solution we found is indeed unique, but only so for constant ρ.

However, even then the freedom of choosing between one of two equivalent angles at the physical boundaries was not fully exploited. The preimage of each physical boundary could contain exactly one or no π turn with an associated outer angle $-\pi$ which permits the preimage of the boundary can still be closed. We can see from the plots that there are points along the boundary where current **changes direction**.

If we consider our solution, which is eventually expressed as a superposition of two solutions from the K_W-space as a **single** solution from **one** K_W that suggests that the according K_W would indeed have such turns for Hall angles $\gamma \in (0, \pi)$.

Going even further back to the assumption ρ be constant, it is an entirely distinct question whether this is in fact a reasonable start. Is the solution unique without that restriction – i.e. is ρ constant the only possible answer to the differential equation? If not, from which physical laws could we infer further boundary conditions so to make the solution unique?

All these questions are not adressed within this report which is confined to solving a Laplace equation with unusual boundary conditions on K_C.

Lastly, the equations in the submanifold's chart took exactly that form because we assumed the map be **isometric** and sufficiently **flat**. What happens for heavily distorted geometries? What would be the shape of the intersection and what would be the effect of the bending on the differential equations?

1. Appendices

1.1. List of Figures

1.2. References

1.2.1. Mathematical background

- *S. Berman and M. Schiffer - Kernel functions and conformal mapping*
- *Wikipedia Foundation et al.*
- *R. F. Wick - Solution of the Field Problem of the Germanium Gyrator*

1.2.2. Software used to solve the problem

- *William A. Stein et al. Sage Mathmematics Software (Version 5.10), The Sage Development Team, 2013, http://www.sagemath.org*
- *The Python Programming Language major version 2 and 3*

1.2.3. Software and standards used to write this

document

- *Inkscape*, an Open Source vector graphics editor
- *VIM* text editor
- *itex2MML itex* to *HTML* precompiler
- *HTML5 W3C* working drafts and standard
- *CSS3 W3C* working drafts and standards
- *Midori WebkitGTK+* based browser
- *Gentoo Linux* linux distribution

1.3. Typesetting this document

This document was written entirely in and in conformance with *HTML 5*, *MathML* and *Cascading Style Sheets*. There are several reasons why the wide spread of documents which are published as *PDF* file should be considered poor practice and rightfully deprecated. Foremost, *PDF* is a compiled document format which means it mangles **semantic content** beyond repair.

Apart from the tiny advantage of text being selectable in *PDF* documents, they are basically the digital cousin of a *print-out*. As of 2013, when this report was written, many **open standards** have reached a mature state and so have their implementations. Standards which retain semantics and are established within the community, such as *HTML 5* should be used to slowly drive relics such as *PDF* out of the world. *Cascading Stylesheets Level 3* are still a work-in-progress and continously improve. Features such as footnotes and fancier paged multi-column layout are in the making, thought not quite production-ready, yet. For the time being, an author is given a set of viable alternatives. They either may realize such features as regular markup (as done in this document), for example manually place footnotes where required, or use one of many precompilers to compile a different language into *HTML* (e.g. *Wikipedia*).

MathML is not eligible to be written directly, because it is *XML* which makes even simple formulas lengthy to write. Instead, formulas can be embedded in the *HTML* code in a *LaTeX* like fashion, delimiting them with dollar-signs from the sourrounding text. The document is then sent through the *itex2MML* precompiler, which outputs the final *HTML* code with the formulas converted to *MathML*.

Also, it is the opinion of the author that *LaTeX*, which is tailored towards producing *PDF* or other compiled content, should be made a thing of the past. The usual argument in favor of *LaTeX* it being ”beautiful” and highly

customizable are misplaced in **sciece**, which is not a fashion show. *TeX* has served its purpose until a few years into the beginning of this century when it was the only reasonable method to typeset documents. In 2013 and onwards, however, all which is left of its former beauty is layers and layers of drying make-up on its wrinkled skin. An enourmous **two gigabytes** delivering but a heinous programming language which has *accumulated* rather than been deliberately designed, over decades.

The scientific community should embrace new, unifying, and powerful concepts which are at the core of today's information technology rather than clinging to the *old ways*. The **open source** movement has unlocked the doors to a better, more structured, and efficient future. It is for us to open them and step through before the hinges rust.